Ain Shams Engineering Journal 15 (2024) 102564

Contents lists available at ScienceDirect

Ain Shams Engineering Journal

journal homepage: www.sciencedirect.com

# A numerical study of initial pressure effects on the water/silver nanofluid interaction with SARS-CoV-2 structure; a molecular dynamics method

Xiaobo Li [a], Dheyaa J. Jasim [b], S. Mohammad Sajadi [c], Guang Fan [a,*], Ameer H. Al-Rubaye [d], Navid Nasajpour-Esfahani [e], Soheil Salahshour [f,g,h], Rozbeh Sabetvand [i]

[a] School of Chemistry and Chemical Engineering, Xianyang Normal University, Xianyang, 712000, China
[b] Department of Petroleum Engineering, Al-Amarah University College, Maysan, Iraq
[c] Department of Nutrition, Cihan University-Erbil, Kurdistan Region, Iraq
[d] Department of Petroleum Engineering, Al-Kitab University, Altun Kupri, Iraq
[e] Department of Materials Science and Engineering, Georgia Institute of Technology, Atlanta 30332, USA
[f] Faculty of Engineering and Natural Sciences, Istanbul Okan University, Istanbul, Turkey
[g] Faculty of Engineering and Natural Sciences, Bahcesehir University, Istanbul, Turkey
[h] Department of Computer Science and Mathematics, Lebanese American University, Beirut, Lebanon
[i] Department of Mechanical Engineering, Islamic Azad University, Iraq

ARTICLE INFO

*Keywords:*
SARS virus
Silver nanoparticles
Nanofluid
Interaction energy
Molecular dynamics simulation

ABSTRACT

The stability of the SARS virus can be affected by various environmental factors, including temperature, humidity, and pressure. In the present research, the effect of initial pressure on the stability of the SARS virus in the presence of water/Ag nanofluid (NF) is investigated using molecular dynamics (MD) simulation. The results revealed that initial pressure effectively changes the atomic evolution of the virus-NF system. Numerically, the diffusion coefficient of modeled samples changes from 32.33 $nm^2$/ns to 9.489 $nm^2$/ns by initial pressure varies from 1 bar to 10 bar. This structural evolution caused interatomic distance and force between virus particle changes. Finally, interaction energy is changed by initial pressure variation, and this parameter varies between −0.44695 kcal/mol to −24.65127 kcal/mol in defined initial conditions. From MD outputs, it was concluded physical stability of the SARS virus in the presence of water/silver NF can be manipulated by initial pressure. So, the SARS virus destruction process with water/silver NF affected from the initial pressure ratio, appropriately. Future directions for this research project may involve exploring the influence of additional environmental factors and utilizing the gained knowledge to develop antiviral materials. This study establishes a foundation for further investigations into the interaction between environmental factors, NFs, and viral infections, with the potential to contribute to the development of effective strategies for combating viral infections and designing innovative antiviral solutions.

## 1. Introduction

Coronaviruses commonly cause infections in both humans and animals. Two major outbreaks of SARS have occurred, resulting in a highly contagious and life-threatening form of pneumonia. Both epidemics occurred between 2002 and 2004 [1,2]. SARS is an airborne virus that spreads similarly to colds and flu. The SARS virus is spread in the air by small saliva droplets coughed or sneezed by an infected person [3]. SARS has flu-like symptoms that usually start 2 to 7 days after infection [4]. This disease causes failure in various organs, including the respiratory, digestive, kidney, and central nervous systems, and the severity of infection with this virus is directly related to the number of receptors in the tissues [5]. The stability, spread, and transmission of the SARS virus depend on many factors, and this has made it one of the most important topics for researchers . therefore, Meyerowitz et al. [6] reviewed the transmission, viral, host, and environmental factors of SARS-CoV-2 virus. Studies have shown that respiratory transmission is predominant, and proximity and ventilation are key factors determining the risk of transmission. Zhang et al. [7] studied the molecular interaction mechanism between SARS-CoV-2 and host cells. In this paper,

*Abbreviations:* MD, Molecular dynamics; CoVs, Coronaviruses; PDB, Protein data bank; NF, Nanofluid; Ag, Silver.

* Corresponding author.
*E-mail addresses:* kythgona@126.com (X. Li), fanguang202309@163.com (G. Fan).

https://doi.org/10.1016/j.asej.2023.102564
Received 10 July 2023; Received in revised form 24 October 2023; Accepted 29 October 2023
Available online 22 November 2023

**Table 1**
The LJ for particles in MD [30,31].

| Particle's type | $\varepsilon_{ij}$ (kcal/mol) | $\sigma_{ij}$ (Å) |
|---|---|---|
| Ag | 0.036 | 3.148 |
| H | 0.010 | 2.852 |
| O | 0.415 | 3.306 |
| C | 0.305 | 3.725 |
| Cl | 0.227 | 3.947 |
| N | 0.415 | 3.561 |
| S | 0.215 | 3.690 |

they reviewed the current knowledge and important information about how SARS-CoV-2 adheres to the surface of host cells through different receptors. Aboubakr et al. [8] studied the Persistence of SARS-CoV-2 and other coronaviruses in the environment and common touch surfaces and the influence of weather conditions. They presented existing data on the persistence of coronaviruses (CoVs), including SARS-CoV-2, from previous reports to help understand its environmental survival.

For instance, Kratzel et al. [9] investigated the Temperature-dependent surface stability of SARS-CoV-2. The results showed that the infection of SARS-CoV-2 was greatly reduced during the initial drying process. However, after that, the virus remains infectious in the dried state for several days regardless of changes in ambient temperature. Kasloff et al. [10] investigated the stability of SARS-CoV-2 in critical conditions of personal protective equipment. Their findings showed that persistence in cotton is greatly reduced. These results emphasize the importance of correctly using personal protective equipment during and after use in high-risk environments to minimize its probability. Mori et al. [11] explained the interactions regulating the structural stability and dynamics of the SARS-CoV-2 S protein. This study elucidated the fundamental mechanisms of structural stability and functional motions of protein S that are relevant for vaccine and antiviral drug development. Morris et al. [12] investigated the effect of temperature and humidity on the stability of SARS-CoV-2 and other enveloped viruses. This study showed that common mechanisms might determine environmental stability for many enveloped viruses. Teng et al. [13]. Investigated the systemic effects of missense mutations on the stability of SARS-CoV-2 spike glycoprotein for developing drugs and vaccines against COVID-19.

In line with the statements above, SARS virus stability and effective parameters, such as environment, temperature, personal equipment, etc., were investigated by numerous researchers. Additionally, numerous types of research on viruses and different materials have been done by MDs to find properties, stability, etc. [14–17]. Yan et al. [18] examined the effects of different boundary wall temperatures on the flow characteristics of fluid flow in microchannels with roughened and smooth surfaces using MD. The results revealed that adding roughness elements on the smooth surface of the microchannel can augment density fluctuation, and increasing wall temperatures empowers the boiling process, which reduces the effect of roughness. Dehkordi et al. [19] examined the effects of electric field and microchannel type on the dynamical behavior of $H_2O/Fe_3O_4$ nanofluid (NF) using MD. The results revealed that the magnitude of the external electric field is a significant parameter in the NF's dynamical behavior in microchannels, with increasing electric field magnitude enhancing the highest rate of velocity, temperature, and density of the NF. Farzinpour et al. [20] the behavior of water/$Fe_3O_4$ NF in the presence of constant and time-dependent magnetic fields using MD. It was observed that NFs

**Table 2**
The MD simulation parameters in the present simulation.

| MD Simulation Setting | Value or Method |
|---|---|
| MD Box Length(A) | $145 \times 145 \times 145$ Å$^3$ |
| Number of Atoms | 9020 |
| Boundary Condition | p p p |
| Initial Temperature | 300 K |
| Thermostat | Nose-Hoover [21,22] |
| Time Step | 0.1 fs |
| Total Simualtion Time | 200,000 fs |

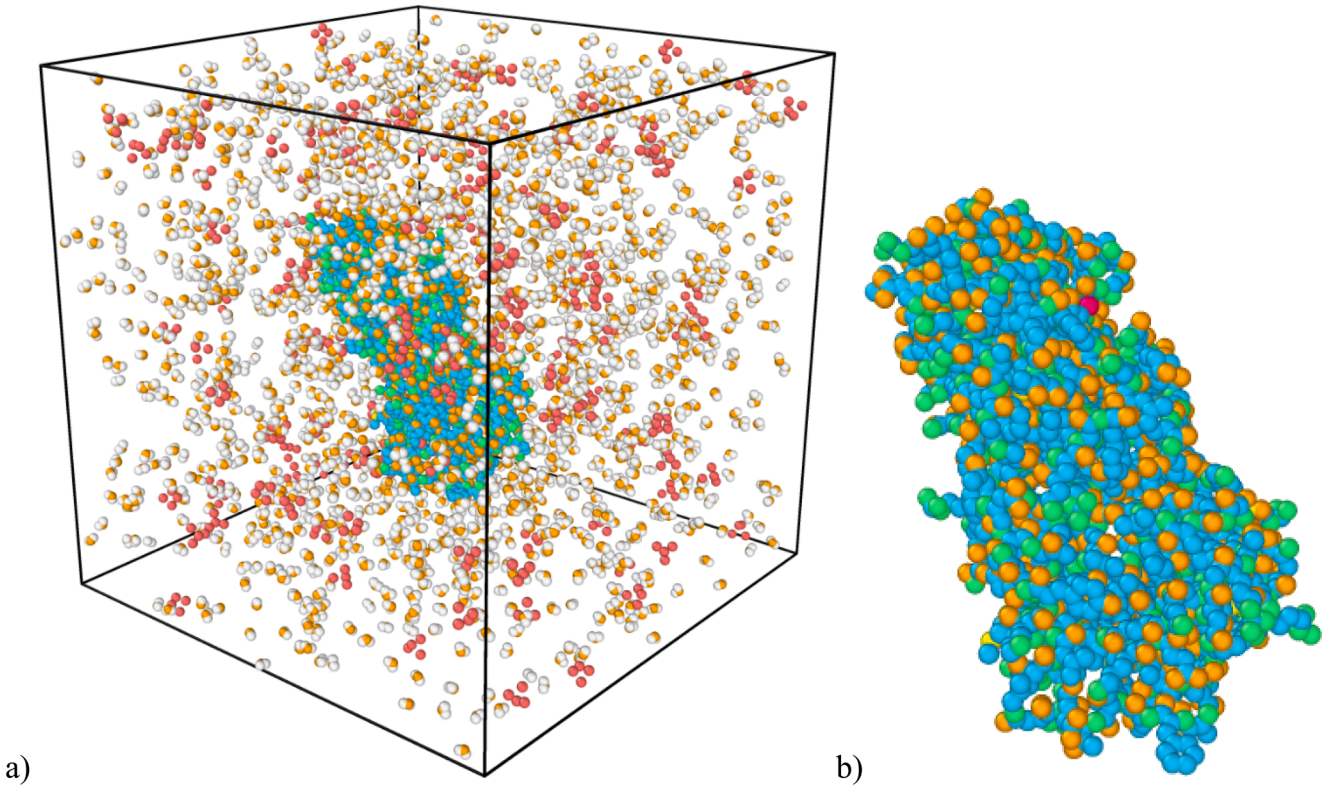


**Fig. 1.** A Schematic of a) simulation box and b) SARS structure.

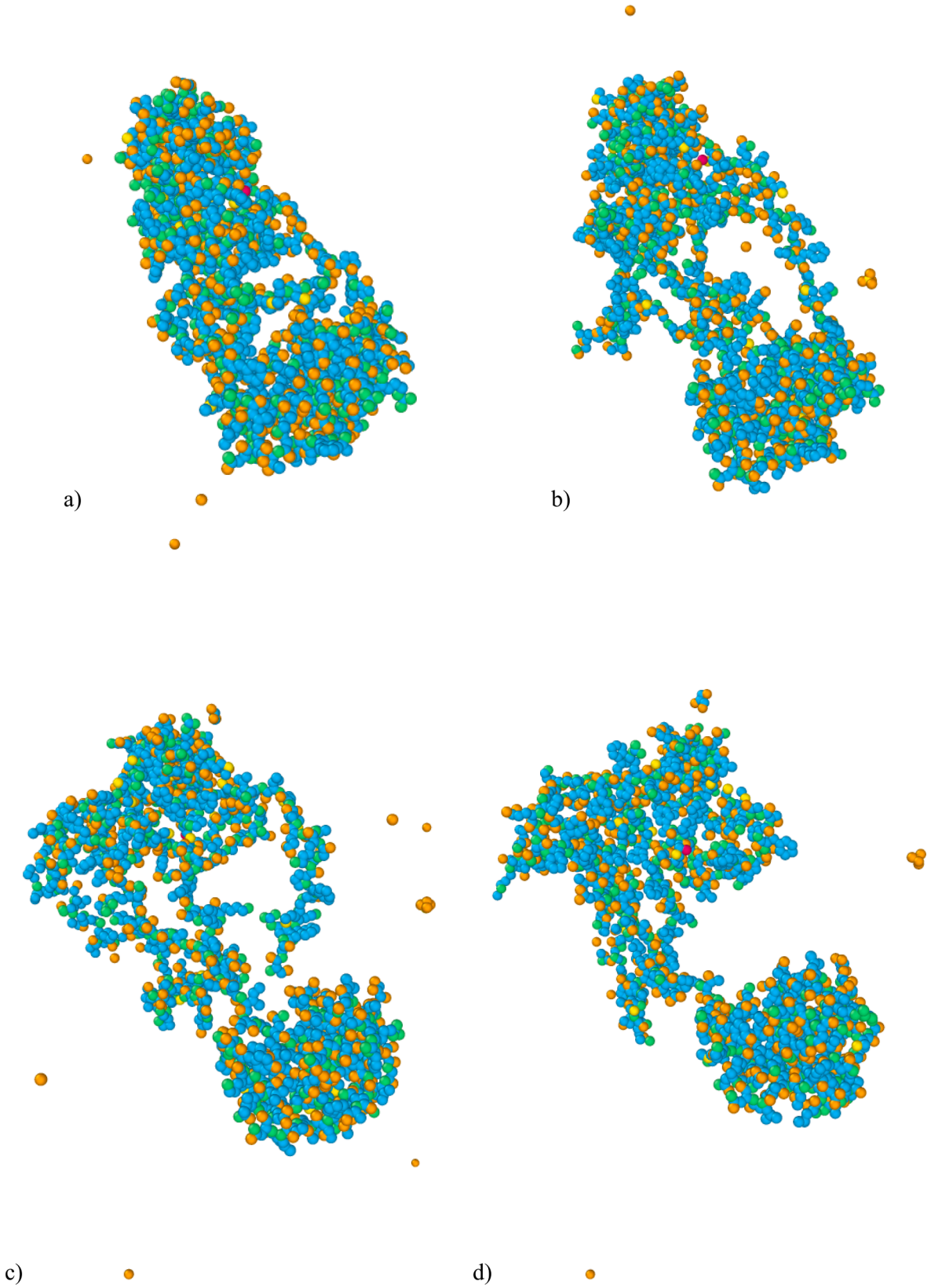


**Fig. 2.** The evolution of SARS structure after a) 250,000, b) 500,000, c) 750,000, and d) 1000,000-time steps.

subjected to magnetic forces agglomerate at a faster rate. MDs offer significant advantages in science, including the ability to predict material properties before experiments, providing detailed insights into atomic and molecular behavior, cost-effectiveness compared to experimental methods, efficient screening of material properties, and facilitating the design of new materials [21,22]. By simulating the behavior of individual atoms and molecules, researchers can save time and resources by predicting material properties, gaining a deeper

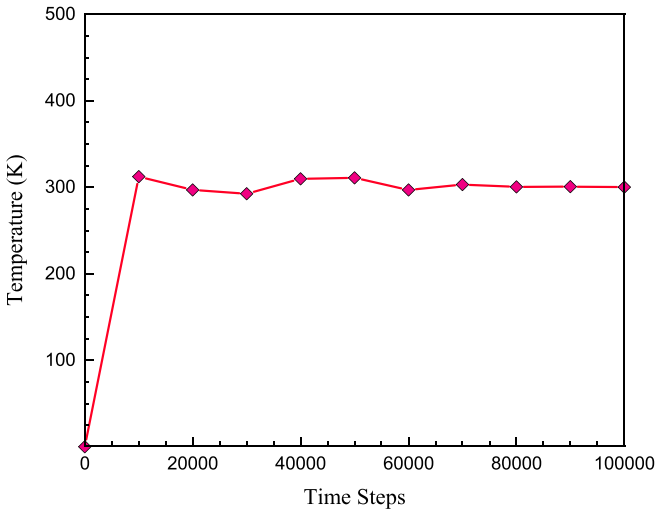


**Fig. 3.** The changes in temperature of simulated structure at 1 bar.

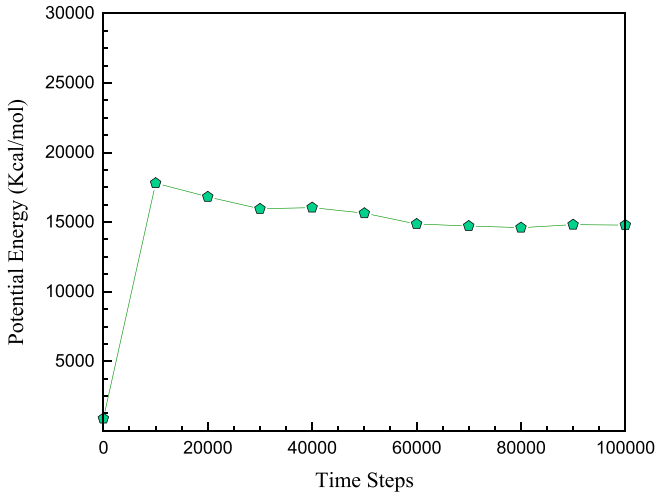


**Fig. 4.** The changes in the potential energy of the structure at 1 bar.

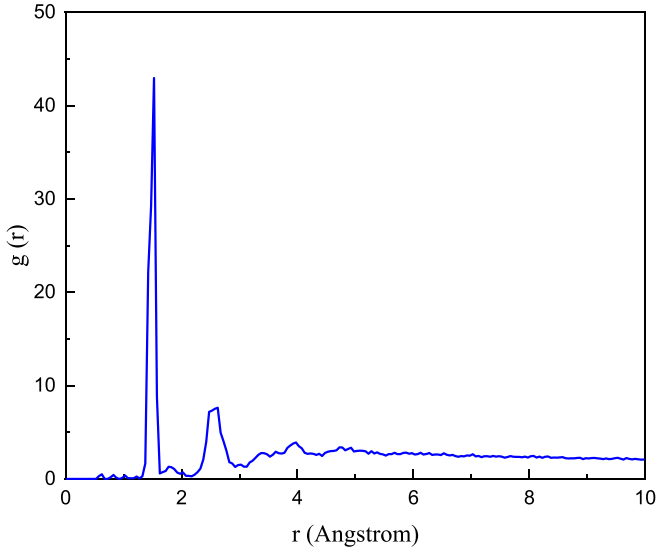


**Fig. 5.** RFD of Sars virous.

understanding of underlying mechanisms, exploring a broader range of conditions, accelerating materials discovery, and tailor materials for specific applications [23]. MDs serve as a powerful tool that enhances scientific research and enables advancements in various fields [24]. In recent research, the effect of initial pressure with different ratios of 1, 2, 3, 5, and 10 bars on water/silver NF interaction with the SARS virus was investigated by MD.

## 2. Simulation

### 2.1. mD

MD is a simulation method to investigate the thermodynamic behavior of materials. This method is related to the force, speed, and location of particles, and the most important factor is power. MD works based on solving Newton's equations of motion [25]:

$$F_i = m_i a_i = -\nabla_i U = -\frac{dU}{dr_i} \tag{1}$$

In this method, a simple algorithm for numerical integration in small time steps is used to analytically describe the movement of particles, which is very difficult due to its coupling nature. One of these algorithms, which is very fast, is called the velocity-Verlet algorithm. The molecular dynamics simulates the displacement and speed of the particles in the simulation box. Using statistical mechanics concepts, the characteristics of the simulated systems are calculated. This algorithm is expressed by the following equations [26,27].

$$r_i\ (\mathrm{t} + \ \Delta \mathrm{t}) = 2\ r_i(t) - \ r_i(t - \ \Delta t) + \left(\frac{d^2 r_i}{dt^2}\right)\ (\Delta t)^2 \tag{2}$$

$$v_i(t + \Delta t) = v_i(t) + \Delta t\ v_i(t) + \frac{\Delta t\ (a_i\ (t) + a_i(t + \Delta t)\ )}{2} \tag{3}$$

The potential function is generally divided into interaction and non-interaction potentials.

Regarding non-bonding potentials, it can be said that there are different types of non-bonding interaction potential energy, and this research used two types of them. One of them was Lennard-Jones [28]:

$$U_{LJ} = 4\varepsilon_{ij}\left[\left(\frac{\sigma_{ij}}{r_{ij}}\right)^{12} - \left(\frac{\sigma_{ij}}{r_{ij}}\right)^{6}\right] \quad r_{ij} < r_c \tag{4}$$

These values are calculated as follows [29]:

$$\varepsilon_{ij} = \sqrt{\varepsilon_i \varepsilon_j} \tag{5}$$

$$\sigma_{ij} = \frac{\sigma_i + \sigma_j}{2} \tag{6}$$

The values of $\varepsilon_{ij}$ and $\sigma_{ij}$ for present particles are listed in Table 1.

### 2.2. Simulation details

In the present paper, the MD method investigated the effect of initial pressure on the water/silver NF interaction with the SARS virus (SARS-COV-2 (VRN1)). First, the protein data bank (PDB) was used to model the SARS structure. Modeling the SARS structure using the PDB was a common approach in structural biology research. By studying the structure of the virus, researchers could gain insights into its behavior and develop strategies for combating it. It's important to note that the stability of the SARS virus can be affected by various environmental factors, including temperature, humidity, pressure, etc. By investigating the effect of initial pressure on the stability of the SARS structure, this paper may contribute to understanding how the virus behaves under different conditions. The water molecules and Ag nanoparticles were modeled using Avogadro software. Avogadro software is popular for modeling molecular structures, including water molecules and Ag

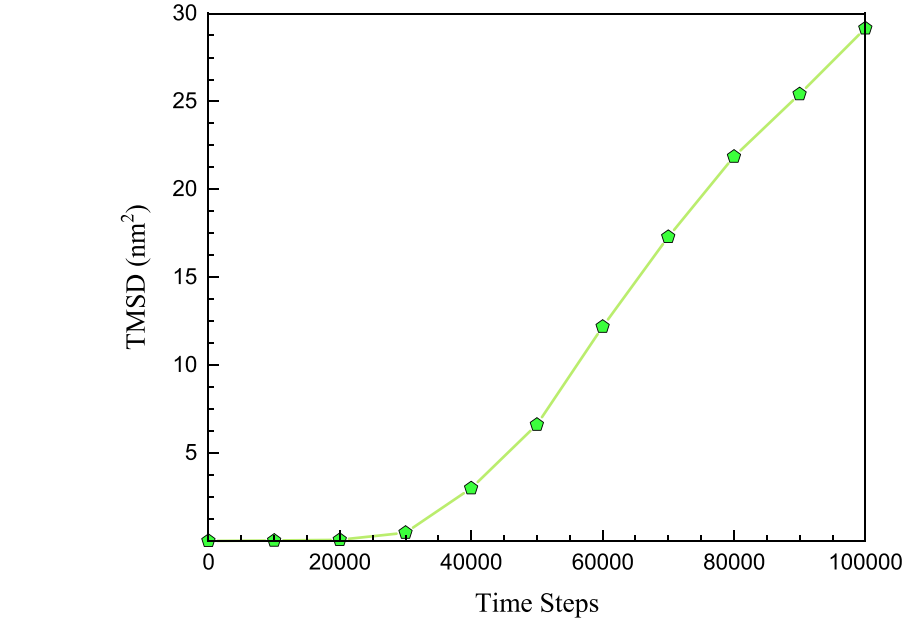


a)

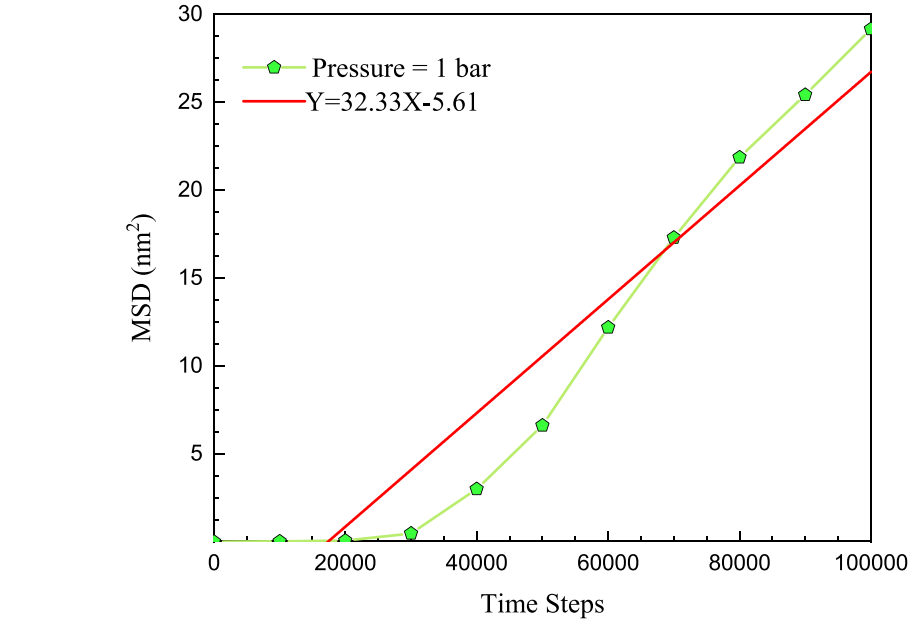


b)

**Fig. 6.** The changes in the a) TMSD and b) diffusion coefficient of the simulated sample at 1 bar.

nanoparticles. Using this software to model the behavior of water molecules and Ag nanoparticles in the context of the SARS virus, researchers can gain insights into how these components interact with the virus and affect its stability. The dimensions of the simulation box set were 145 Å. The boundary conditions are periodic in all directions. Fig. 1 demonstrates a schematic of the simulation box and SARS structure. After modeling, the equilibrium of the simulated structure was done by checking changes in temperature and potential energy. In this step, the NPT ensemble is used. The initial temperature and pressure are set to 300 K and 1 bar (See Table 2).

After that, the ensemble changed to NVE, and the stability of the SARS structure at different pressures was investigated. Fig. 2 shows the evolution of the SARS structure during the simulation after various time steps.

### 2.3. *Equilibrium process*

Temperature and potential energy changes were attended to thermodynamic balance in the first step of equilibrium. These physical parameters outputs for the virus-NF system are depicted in Figs. 3 and 4.

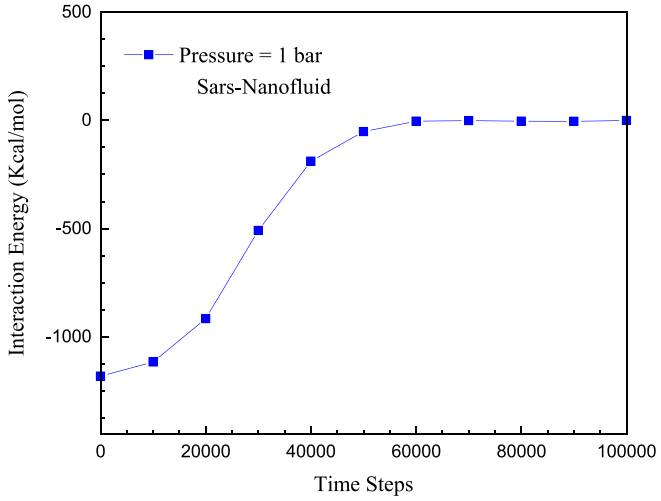


**Fig. 7.** The changes in the interaction energy of SARS-NF at 1 bar.

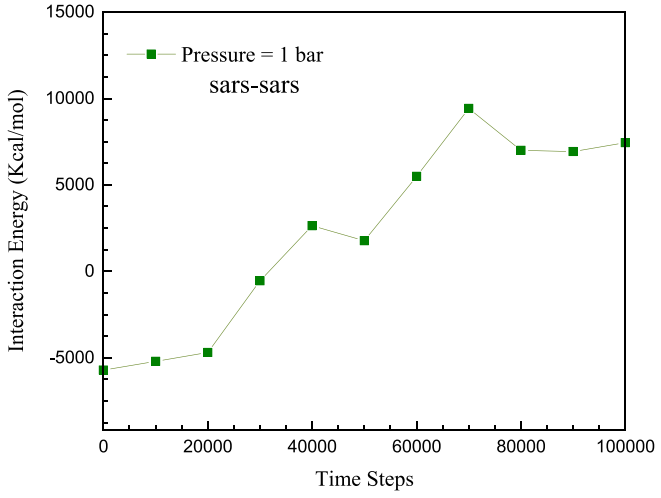


**Fig. 8.** The changes in the interaction energy of SARS-SARS at 1 bar.

The changes in temperature of the system converged to 300 K (as the initial temperature) after 100000-time steps, as shown in Fig. 3. This calculation predicted the 100000-time steps were sufficient for equilibrium phase detection in the modeled sample. Furthermore, potential energy shows similar behavior. As shown in Fig. 4, potential energy converged to 14790.256 kcal/mol after 100,000-time steps. Physically, this convergence of energy is obtained from the force of attraction between different atoms in defined initial conditions. Technically, this behavior predicted appropriate MD settings inside the computational box, as reported in previous research [32–34].

## 3. Validation

After equilibrium phase detection in the defined initial condition for the SARS virus, the validation process of the MD method is done via radial distribution function calculation (RDF). Computationally, this function describes the arrangement of the particles in atom-base samples. RDF is a mathematical function that describes the probability of finding a particle at a certain distance from a reference particle or group of particles. It is commonly used in the field of molecular dynamics and materials science to analyze the spatial arrangement of particles in a system. Fig. 5 represents the RDF of the SARS virus after the equilibration process. Our calculated pattern for the RDF parameter of the SARS virus is depicted in Fig. 5. The Calculated pattern for the SARS virus nanostructure is consistent with various reports on the SARS virus nanostructure at constant temperature [34].

## 4. Results and discussion

After equilibrium phase detection in the virus-NF system, the system's evolution was reported using the NVE ensemble for 100000-time steps. TMSD, diffusion coefficient, and interaction energy outputs are reported in this section. It is calculated by squaring the distance traveled by the particle at each time interval, averaging these values over all time intervals, and then taking the square root of the result. Mean square displacement is widely used in physics and chemistry to characterize particle behavior in various systems, from simple liquids to complex biological systems. TMSD and diffusion coefficient results at standard conditions are depicted in Fig. 6. MD outputs predicted by simulation time passing, the atomic fluctuations enlarged, and the TMSD parameter converged to 29.16 $nm^2$. This atomic evolution caused the diffusion coefficient to converge to 32.33 $nm^2$/ns after 100000-time steps. Physically, the diffusion coefficient increasing shows SARS virus destruction in defined conditions.

The structural evolution of atomic systems arises from their interaction energy. The interaction energy between virus particles and virus-NF particles was calculated to analyze this parameter. These results are depicted in Figs. 7 and 8. These interaction energies decrease with simulation time passing. In other words, this evolution was obtained from virus particle distribution in larger distances in the modeled system. Based on figures, the interaction energy between SARS and water/silver NF decreased to −0.44695 kcal/mol after 100000-time steps. This parameter converged to 7444.9051 kcal/mol for SARS particles. From these outputs, we concluded NF particle diffusion to the target virus caused an effective collision between this biological sample's particles and increased the mean distance between them.Fig. 8.

The initial pressure inside the computational box causes the amplitude of various structures to change effectively. This structural evolution decreased the physical stability of the virus. To report this initial parameter effects on the SARS virus destruction process, the initial pressure changes from 1 bar to 10 bar. As shown in Fig. 9, by initial pressure increasing to 10 bar, the TMSD parameter converged to 7.12 $nm^2$. This evolution caused the ratio of NF particle diffusion to pristine virus and diffusion coefficient. Numerically, the diffusion coefficient converges to 9.489 $nm^2$/ns after a 100000-time step in the system with a 10 bar pressure setting. Physically, by increasing pressure, the sample's total volume decreases to a lesser ratio, and vacant regions inside the sample decreased. Finally, these vacant regions decreases, enlarged the repulsive force inside the SARS virus, and the stability of this sample decreased against water/silver NF.

The interaction energy of various modeled parts is reported in this section in Figs. 10 and 11 to analyze the pressure effect on the physical stability of the SARS virus in the vicinity of water/silver NF. The interaction energy changes between the virus and NF as a function of initial pressure are depicted in Fig. 10. Numerically, this parameter decreased to −3.41360 value in 10 bar. This atomic evolution caused interatomic distance to decrease inside the modeled virus, creating repulsive force inside the sample, and their physical stability decreased. So, we concluded the system's physical stability decreased with increasing pressure, and SARS destruction effectively occurred at higher pressures. Similar performance was detected in the interaction energy between virus particles. Numerically, this parameter changed from −0.44695 kcal/mol to −24.65127 kcal/mol in the presence of various initial pressures. Our numerical results in this section are listed in Table 3. Finally, we concluded that the initial pressure could be an effective parameter in the destruction process of the SARS virus in clinical applications and should be supposed in actual cases..

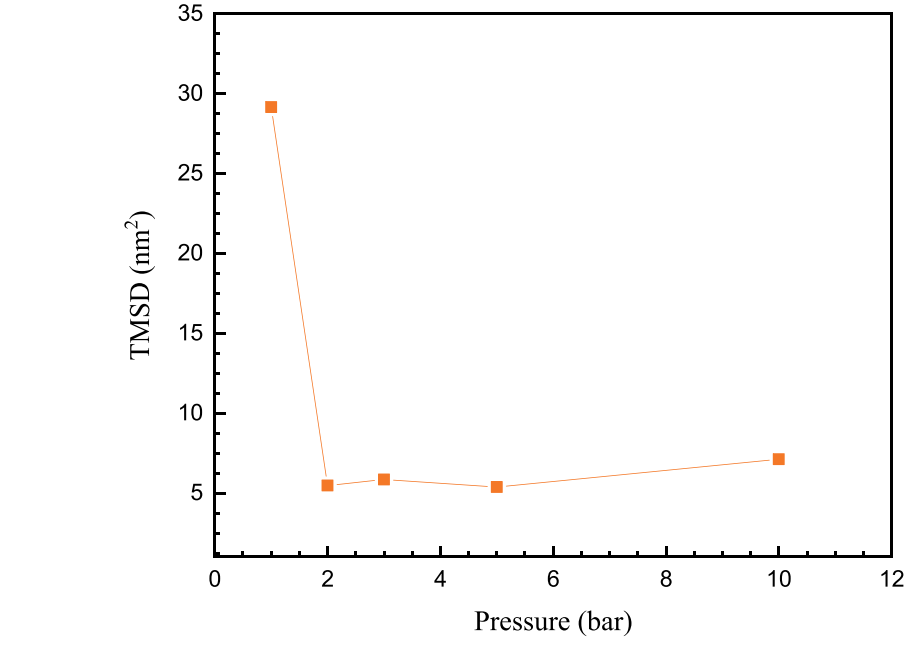


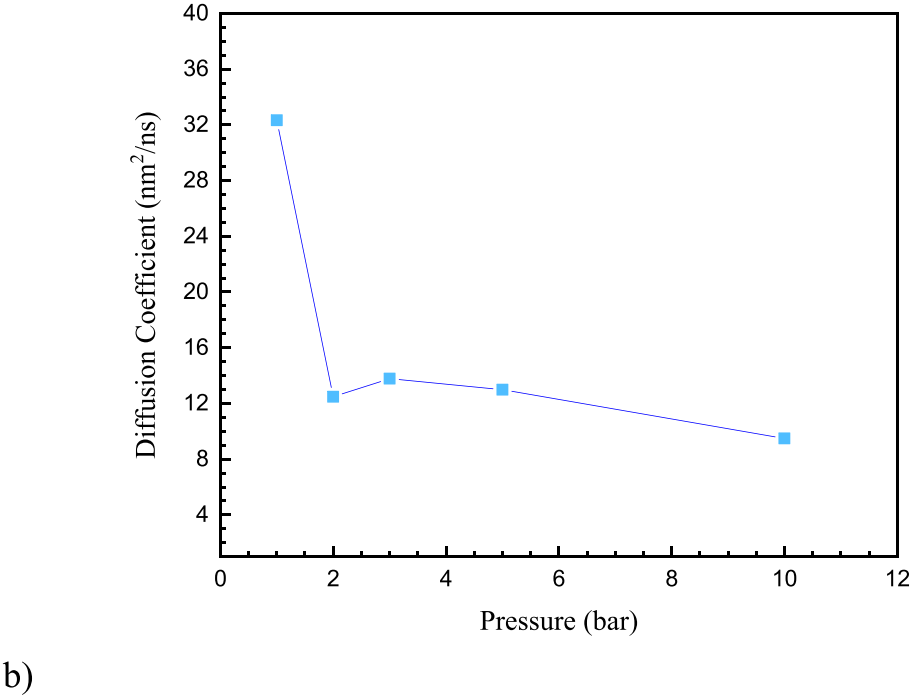


**Fig. 9.** The changes in the a) TMSD and b) diffusion coefficient of the simulated sample with different pressure ratios.

## 5. Conclusion

In the present research, we designed water/silver NF for the SARS virus destruction process in clinical cases using the molecular dynamics (MD) approach. The novelty in this study is the use of a water/silver NF for the destruction of the SARS virus, which has not been extensively studied for this purpose. Additionally, the introduction of initial pressure changes as a means of enhancing the destruction process is a novel approach. Equilibrium phase simulations show temperature and potential energy convergence to 300 K and 14790.256 kcal/mol (respectively) after 100000-time steps. This convergence validated the MD method to study SARS virus-water/silver NF in equilibrium conditions. After equilibrium phase detection in modeled samples, the destruction process of the SARS virus is introduced by initial pressure changes. For this purpose, various physical parameters such as total mean square displacement (TMSD), diffusion coefficient, and interaction energy were calculated. Numerical outputs show the diffusion coefficient changes from 32.33 nm$^2$/ns to 9.489 nm$^2$/ns by initial pressure

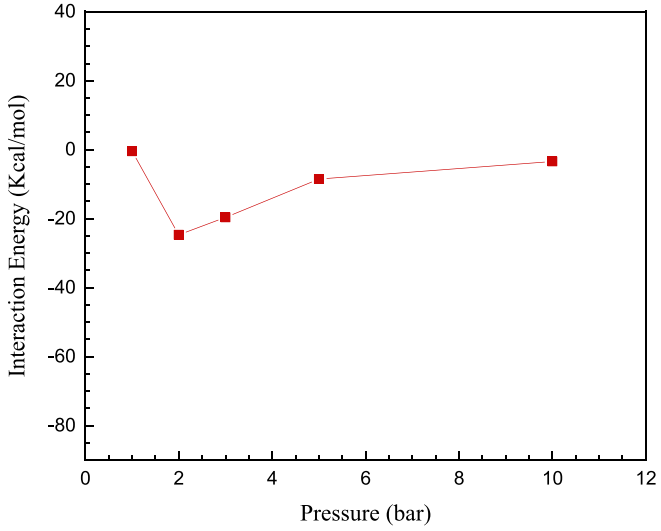


**Fig. 10.** The changes in the interaction energy of the SARS-NF sample with different pressure ratios.

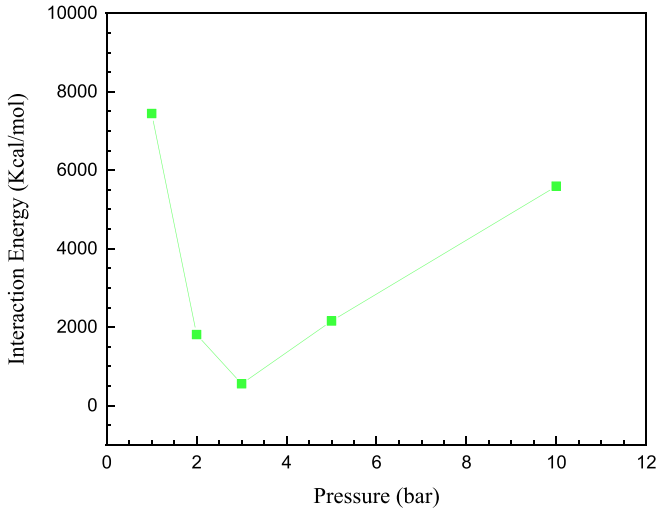


**Fig. 11.** The changes in the interaction energy of the SARS-SARS sample with different pressure ratios.

**Table 3**
The SARS virus's numerical changes in TMSD, diffusion coefficient, and interaction energy at a different initial pressure.

| Pressure (bar) | TMSD ($nm^2$) | Diffusion coefficient ($nm^2$/ns) | Interaction Energy (kcal/mol) | |
|---|---|---|---|---|
| | | | SARS-NF | SARS-SARS |
| 1 | 29.16 | 32.33 | −0.44695 | 7444.9051 |
| 2 | 5.47 | 12.48 | −24.65127 | 1811.3268 |
| 3 | 5.85 | 13.78 | −19.63726 | 557.41415 |
| 5 | 5.38 | 12.98 | −8.52769 | 2155.1598 |
| 10 | 7.12 | 9.489 | −3.4135964 | 5592.8549 |

variation from 1 bar to 10 bar. This structural evolution caused interaction energy changes from −0.44695 kcal/mol to −24.65127 kcal/mol inside the modeled sample. From these numerical results, we concluded water/silver NF is a promising mixture for the SARS virus destruction process. These findings have significant implications for developing effective antiviral treatments in clinical settings.

## 6. Future outline

In conclusion, this research project provides valuable insights into the potential use of water/silver NF for the destruction of the SARS virus in clinical cases. Future directions include optimization of NF composition, in vivo studies, scale-up and manufacturing, and clinical trials. These efforts would provide concrete evidence of the effectiveness and safety of water/silver NFs, as well as insights into the broader field of NFs and their applications in healthcare. If successful, this research project could contribute significantly to the development of innovative antiviral strategies and materials for combating viral infections, ultimately benefiting public health and improving clinical treatments.

## Declaration of Competing Interest

The authors declare that they have no known competing financial interests or personal relationships that could have appeared to influence the work reported in this paper.

## References

[1] Martina BE, Haagmans BL, Kuiken T, Fouchier RA, Rimmelzwaan GF, Van Amerongen G, et al. SARS virus infection of cats and ferrets. Nature 2003;425(6961):915.
[2] Li J, Lai S, Gao GF, Shi W. The emergence, genomic diversity and global spread of SARS-CoV-2. Nature 2021;600(7889):408–18.
[3] Senatore V, Zarra T, Buonerba A, Choo K-H, Hasan SW, Korshin G, et al. Indoor versus outdoor transmission of SARS-COV-2: environmental factors in virus spread and underestimated sources of risk. Euro-Mediterranean Journal for Environmental Integration 2021;6:1–9.
[4] Chung E, Chow EJ, Wilcox NC, Burstein R, Brandstetter E, Han PD, et al. Comparison of symptoms and RNA levels in children and adults with SARS-CoV-2 infection in the community setting. JAMA Pediatr 2021;175(10).
[5] Zhang Q, Wang Y, Bai RT, Lian BR, Zhang Y, Cao LM. X-linked Charcot-Marie-Tooth disease after SARS-CoV-2 vaccination mimicked stroke-like episodes: A case report. World journal of clinical cases 2023;11(2):464–71. https://doi.org/10.12998/wjcc.v11.i2.464.
[6] Meyerowitz EA, Richterman A, Gandhi RT, Sax PE. Transmission of SARS-CoV-2: a review of viral, host, and environmental factors. Ann Intern Med 2021;174(1):69–79.
[7] Zhang Q, Xiang R, Huo S, Zhou Y, Jiang S, Wang Q, et al. Molecular mechanism of interaction between SARS-CoV-2 and host cells and interventional therapy. Signal Transduct Target Ther 2021;6(1):233.
[8] Aboubakr HA, Sharafeldin TA, Goyal SM. Stability of SARS-CoV-2 and other coronaviruses in the environment and on common touch surfaces and the influence of climatic conditions: a review. Transbound Emerg Dis 2021;68(2):296–312.
[9] Kratzel A, Steiner S, Todt D, V'kovski P, Brueggemann Y, Steinmann J, et al. Temperature-dependent surface stability of SARS-CoV-2. J Infect 2020;81(3):452–82.
[10] Kasloff SB, Leung A, Strong JE, Funk D, Cutts T. Stability of SARS-CoV-2 on critical personal protective equipment. Sci Rep 2021;11(1):1–7.
[11] Mori T, Jung J, Kobayashi C, Dokainish HM, Re S, Sugita Y. Elucidation of interactions regulating conformational stability and dynamics of SARS-CoV-2 S-protein. Biophys J 2021;120(6):1060–71.
[12] Morris DH, Yinda KC, Gamble A, Rossine FW, Huang Q, Bushmaker T, et al. Mechanistic theory predicts the effects of temperature and humidity on inactivation of SARS-CoV-2 and other enveloped viruses. Elife 2021;10:e65902.
[13] Teng S, Sobitan A, Rhoades R, Liu D, Tang Q. Systemic effects of missense mutations on SARS-CoV-2 spike glycoprotein stability and receptor-binding affinity. Brief Bioinform 2021;22(2):1239–53.
[14] Choi K-E, Kim J-M, Rhee J, Park AK, Kim E-J, Kang NS. Molecular Dynamics Studies on the structural characteristics for the stability prediction of SARS-CoV-2. Int J Mol Sci 2021;22(16):8714.
[15] Ghahremanian S, Rashidi MM, Raeisi K, Toghraie D. Molecular dynamics simulation approach for discovering potential inhibitors against SARS-CoV-2: A structural review. J Mol Liq 2022:118901.
[16] Liu X, Ghafari B, Patra I, Kadhim MM, Turki Jalil A, Kumar Anil, et al. A molecular dynamics study of thermal behavior of ammonia/Cu nanorefrigerant flow under different initial pressures and electric fields. Journal of Molecular Liquids 2022;367(120388):120388. https://doi.org/10.1016/j.molliq.2022.120388.
[17] Liu X, Patra I, Kuzichkin OR, Zaidi M, Abdulnabi SM, Mohsen Najm Z, et al. Molecular dynamics study of the effect of external electric field amplitude and cavity on thermal properties of Ammonia/Copper Nano-Refrigerant. Journal of Molecular Liquids 2022;365(120125):120125. https://doi.org/10.1016/j.molliq.2022.120125.
[18] Yan S-R, Shirani N, Zarringhalam M, Toghraie D, Nguyen Q, Karimipour A. Prediction of boiling flow characteristics in rough and smooth microchannels using molecular dynamics simulation: Investigation the effects of boundary wall temperatures. J Mol Liq 2020;306:112937.

[19] Ghani Dehkordi K, Karimipour A, Afrand M, Toghraie D, Meghdadi Isfahani AH. The electric field and microchannel type effects on H 2 O/Fe 3 O 4 nanofluid boiling process: molecular dynamics study. Int J Thermophys 2020;41:1–17.
[20] Farzinpour M, Toghraie D, Mehmandoust B, Aghadavoudi F, Karimipour A. Molecular dynamics simulation of ferronanofluid behavior in a nanochannel in the presence of constant and time-dependent magnetic fields. J Therm Anal Calorim 2020;141(6):2625–33.
[21] Krieger E, Vriend G. New ways to boost molecular dynamics simulations. J Comput Chem 2015;36(13):996–1007.
[22] Bernardi RC, Melo MC, Schulten K. Enhanced sampling techniques in molecular dynamics simulations of biological systems. Biochimica Et Biophysica Acta (BBA)-General Subjects 2015;1850(5):872–7.
[23] Glotzer SC, Paul W. Molecular and mesoscale simulation methods for polymer materials. Annu Rev Mat Res 2002;32(1):401–36.
[24] Hospital A, Goñi JR, Orozco M, Gelpí JL. Molecular dynamics simulations: advances and applications. In: Advances and Applications in Bioinformatics and Chemistry; 2015. p. 37–47.
[25] Rapaport DC, Rapaport DCR. The art of molecular dynamics simulation. Cambridge University Press; 2004.
[26] Verlet L. Computer“ experiments” on classical fluids. I. Thermodynamical properties of Lennard-Jones molecules. Phys Rev 1967;159(1):98–103.
[27] Spreiter Q, Walter M. Classical molecular dynamics simulation with the Velocity Verlet algorithm at strong external magnetic fields. J Comput Phys 1999;152(1):102–19.
[28] Lennard-Jones JE. Cohesion. Proc Phys Soc 1931;43(5):461–82.
[29] Berendsen HJC, Grigera JR, Straatsma TP. The missing term in effective pair potentials. J Phys Chem 1987/11/01, 1987.;91(24):6269–71.
[30] Rappé AK, Casewit CJ, Colwell K, Goddard III WA, Skiff WM. UFF, a full periodic table force field for molecular mechanics and molecular dynamics simulations. J Am Chem Soc 1992;114(25):10024–35.
[31] Mayo SL, Olafson BD, Goddard WA. DREIDING: a generic force field for molecular simulations. J Phys Chem 1990;94(26):8897–909.
[32] Hekmatifar M, Toghraie D, Khosravi A, Saberi F, Soltani F, Sabetvand R, et al. The study of asphaltene desorption from the iron surface with molecular dynamics method. J Mol Liq 2020;318:114325.
[33] Ghanbari A, Warchomicka F, Sommitsch C, Zamanian A. Investigation of the oxidation mechanism of dopamine functionalization in an AZ31 magnesium alloy for biomedical applications. Coatings 2019;9(9):584.
[34] https://www.rcsb.org/structure/7RN1.